



## Static Characterization of Arbitrary Waveform Generator based on Modified Multi-sine Fitting and Zero Crossing Detection Algorithms

Domenico Luca Carni

Dept. of Computer Science, Modelling, Electronics and System, University of Calabria, Ponte P. Bucci 41C, Rende (CS), Italy

Received 27 February 2017; Accepted 22 June 2017

### Abstract

The static characterization of the output section of the Arbitrary Waveform Generator (AWG) requires that its output signal must be digitalized by Analog to Digital Converter (ADC) with higher linearity and resolution than the device under test. In the literature, the problem of high resolution acquisition is translated to the simpler problem of low resolution and high sampling frequency acquisition of the resulting signal, difference between the AWG output signal and the sinusoidal reference signal, available at the output of differential amplifier.

The research is devoted to improving the evaluation accuracy of the AWG output by taking into consideration the degradation causes arising from (i) the delay introduced by the differential amplifier, and (ii) the jitter and other noise sources affecting the detection of the Zero Crossing Time Sequence (ZCTS) in the resulting signal. In the paper a method is proposed based on the processing of the resulting signal, only, and the improved ZCTS detection. Numerical tests validate the proposed method.

*Keywords:* AWG characterization, DAC static testing, AWG transfer characteristic evaluation.

### 1. Introduction

The output section of the AWG is made up of the cascade of high resolution Digital to Analog Converter (DAC) and reconstruction analog filter. The output characteristic of the AWG is that of the cascade of the DAC and the reconstruction filter. The test requires that the AWG output signal is acquired by higher resolution and linearity than the device under test [1].

Among the methods proposed in the literature for the AWG and more in general DAC test [1]–[11], the methods [9],[10] are related to the built-in test implementation. In [11] the scheme of sigma delta modulator is used to detect the non linearity. In [1],[3] the reference signal is obtained by filtering the same input signal and its accuracy is related to the narrow band of the filter and the compensation of the delay introduced by the filter. In [6] the maximum likelihood estimation is used on the signal with superimposed dither noise. In [4] is considered the dynamic parameters estimation and not the static. In general, these methods are characterized by difficult practical implementation due to the additional instrumentation required by the test. However, the method proposed in [2] translates the high resolution requirement to the simpler requirement of high sampling rate. This test method has the advantage of overcoming the difficulty of operating with acquisition systems characterized by both higher resolution and linearity than the AWG under test. The AWG output signal is reconstructed by detecting the Zero Crossing Time Sequence (ZCTS) in the resulting signal, obtained at the output of differential amplifier as the difference between the output signal of the AWG and the sinusoidal reference signal. The accuracy of

the reconstructed signal is closely determined by the estimation accuracy of both the reference signal parameters and the ZCTS.

The research given is devoted to improve accuracy in the evaluation of the AWG output with respect to [2]. Interest is focused on the problems arising from (i) the delay introduced by the differential amplifier, and (ii) the jitter and other noise sources affecting the detection of the ZCTS. The differential amplifier introduces a propagation delay between input and output in the order of hundreds of ns [12],[13] according to the hardware characteristics. Therefore, the resulting signal and the reference signal are not synchronized at the output. They are affected by a time offset that reduces the reconstruction accuracy of the AWG output. Moreover, the noise superimposed on the resulting signal introduces fluctuation in the neighbour of the zero code making the ZCTS estimation inaccurate.

In order to overcome these problems an improved method is proposed in the paper that uses only the resulting signal, and consequently one input channel of the acquisition system, avoiding the effects arising from the delay between the resulting and the reference signal. In particular, the parameters of the reference signal are estimated by the modified version of the multi-sine fitting algorithm [14]–[18] applied to the resulting signal.

Moreover, the improved ZCTS method, with respect to that used in [2], is pointed out. This method uses the linear regression function of the samples in the neighbour of the sign change to detect the zero crossing, so as the fluctuation due to the jitter and noise sources are negligible.

The paper is organized as follows: preliminarily, the basis of the static AWG characterization by sinusoidal reference signal is described and the modified multi-sine fitting algorithm is presented; successively, the improved ZCTS method is described and compared with other method presented in [2]; numerical tests are discussed to assess the improvements of the method for AWG

\*E-mail address: [dlcarni@imes.unical.it](mailto:dlcarni@imes.unical.it)

ISSN: 1791-2377 © 2017 Eastern Macedonia and Thrace Institute of Technology. All rights reserved.

doi:10.25103/jestr.103.03

transfer characteristic reconstruction; experimental test are included to prove the achievable results; finally, the conclusions follow.

## 2. Static AWG Characterization by Sinusoidal Reference Signal

Fig.1 shows the instrument connection to characterize the AWG according to the proposed method. The AWG is set to generate the low frequency sinusoidal signal  $y_{AWG}$ . The latter is subtracted from the reference sinusoidal signal  $y_{REF}$ . The resulting signal  $y_{RS}$  is:

$$y_{RS}(t) = y_{REF}(t) - y_{AWG}(t) = A_{REF} \sin(2\pi f_{REF}t + \phi_{REF}) + C - y_{AWG}(t) \quad (1)$$

where

$A_{REF}, f_{REF}$  and  $\phi_{REF}$  are the amplitude, the frequency and the phase of the reference signal, respectively, and C is the offset. The resulting signal is digitized by ADC and stored and processed into a PC.

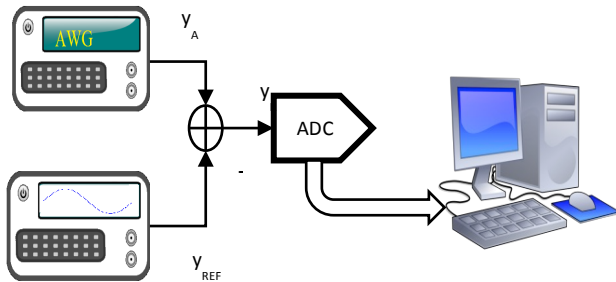


Fig.1. Instrument connection according to the proposed method.

In [2] was proposed to infer the AWG output from knowledge of the reference signal parameters  $A_{REF}, f_{REF}$  and  $\phi_{REF}$ , and the ZCTS estimated on the resulting signal. The advantage is that the resolution of the ADC does not influence the reconstruction of the AWG output because the latter is determined by the ZCTS and the evaluation of the reference signal parameters.

In [2] the resulting signal and the reference one are acquired by two channels, one connected to the AWG output and the other to the differential amplified output. However, the hardware implementing the difference between the reference and AWG signal introduces propagation delay. Then the reference and the resulting signals are not synchronized at the input of the acquisition board, consequently, the reconstruction accuracy of the AWG output signal would be decreased.

To overcome this problem, the processing method [2] is improved according to the block scheme of Fig.2. The resulting signal is processed by the multi-sine fitting algorithm (MSFA) to evaluate the parameters of the reference signal, with accuracy comparable with the method based on Fourier transform [19] and without the problems arising from the spectral leakage in non-coherent sampled signal. Moreover, the zero-crossing detection algorithm modified to operate on low amplitude resolution signal evaluates the ZCTS. The reconstructed AWG output signal  $y'_{AWG}$  is processed to estimate the transfer characteristic and the non-linearity of the AWG.

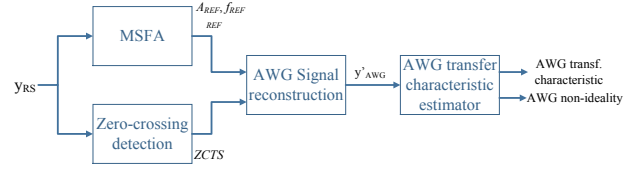


Fig.2. Block scheme of the method for the AWG static characterization.

### 2.1. Modified Multi-sine fitting algorithm

By considering M samples of  $y_{RS}$  with sampling period  $T_c$ , it is:

$$y_{RS} = [y_1, y_2, \dots, y_M]^T \quad (2)$$

The signal (1) can be re-written as:

$$y_{RS} = D x \quad (3)$$

where the vector  $x$  is:

$$x = [A_{LAWG}, A_{QAWG}, A_{IREF}, A_{QREF}, C]^T \quad (4)$$

where  $A_{LAWG}, A_{QAWG}$  are the in-phase and in-quadrature components of the AWG signal,  $A_{IREF}, A_{QREF}$  the in-phase and in-quadrature components of the reference signal, and the matrix  $D$  is:

$$D = \begin{bmatrix} \sin(2\pi f_{AWG}^1 t_1) & \cos(2\pi f_{AWG}^1 t_1) & \sin(2\pi f_{REF}^1 t_1) & \cos(2\pi f_{REF}^1 t_1) & 1 \\ \sin(2\pi f_{AWG}^2 t_2) & \cos(2\pi f_{AWG}^2 t_2) & \sin(2\pi f_{REF}^2 t_2) & \cos(2\pi f_{REF}^2 t_2) & 1 \\ \vdots & \vdots & \vdots & \vdots & \vdots \\ \sin(2\pi f_{AWG}^M t_M) & \cos(2\pi f_{AWG}^M t_M) & \sin(2\pi f_{REF}^M t_M) & \cos(2\pi f_{REF}^M t_M) & 1 \end{bmatrix} \quad (5)$$

$f_{AWG}$  is the frequency set in the AWG for the generation of sinusoidal signal. The multi-sine signal parameters  $\hat{x}$ , which minimize the least square error between the acquired samples (2) and the reconstructed ones, can be estimated as the solution of the overdetermined linear system [20]:

$$\hat{x} = [D^T D]^{-1} D^T y_{RS} \quad (6)$$

From  $\hat{A}_{IREF}, \hat{A}_{QREF}$ , extracted by  $\hat{x}$  of (6), the amplitude  $\hat{A}_{REF}$  and phase  $\hat{\phi}_{REF}$  of the reference signal are:

$$\hat{A}_{REF} = \sqrt{\hat{A}_{IREF}^2 + \hat{A}_{QREF}^2} \quad \hat{\phi}_{REF} = \text{atan} \frac{\hat{A}_{QREF}}{\hat{A}_{IREF}} \quad (7)$$

### 2.2 Improved ZCTS

The problem of zero-crossing detection is interesting topic addressed in the literature [21]–[25]. However, most of the methods require the signal to be acquired by high resolution ADC. In the case under examination, the signal is oversampled, corrupted by noise and acquired by low resolution ADC. Most of the methods fail because there are more samples equal to zero in the neighbour of the awaited zero crossing. The noise causes fluctuation around the zero crossing of the signal in unpredictable way. To overcome this difficulty, the new method is proposed based on the block scheme of Fig.3.

The method analyses the samples inside a sliding window of constant size, which is shifted on the signal. The size of the

window is lower than half of the reference signal semi-period. The main steps of the method are:

1. if it is recognized that the samples of (2) included in the window have different sign, then the zero crossing is included in the window. The method uses linear regression in the neighbour of the sign change, defined by the samples included in  $\pm 3$  codes from the 0 code, as shown in Fig.4. The linear regression is justified by the fact that the signal is oversampled and it can be assumed as linear inside the neighbour of sign change of the samples.
2. estimated the parameters of the linear regression, the zero-crossing time is detected;

**2.3. Signal reconstruction based on ZCTS and sinusoidal reference signal**

By  $A_{REF}$ ,  $f_{REF}$  and  $\phi_{REF}$  and the ZCTS  $t_i$ ,  $i=1, \dots, N$ , of the signal (2),  $y_{AWG}$  is reconstructed.

The method takes into consideration that in ZCTS is:

$$y_{REF}(t_i) - y_{AWG}(t_i) = A_{REF} \sin(2\pi f_{REF} t_i + \phi_{REF}) - y_{AWG}(t_i) = 0, \quad i=1, \dots, N \quad (8)$$

From (8)  $y_{AWG}$  is evaluated as:

$$y_{AWG}(t_i) = A_{REF} \sin(2\pi f_{REF} t_i + \phi_{REF}) \quad (9)$$

The N samples of the ZCTS are non-uniformly distributed in the time domain. By the way, if the reference signal has amplitude higher than that of the AWG output, each semi-period of the reference signal forces a zero crossing. Therefore, for the successive analysis of the reconstructed signal, it is imposed that the frequency of the reference signal must be at least 100 times higher than the AWG signal, and that the ratio between  $f_{AWG}$  and  $f_{REF}$  is not an integer. In this way, the ZCTS of the resulting signal are related to different codes of the AWG in each period of  $y_{AWG}$  [26]. The same shrewdness is used in setting the ratio between the  $f_{REF}$  and the ADC sampling frequency. In this way, each acquired sample corresponds to a different phase of the reference signal and the multi-sine fitting algorithm has more information to operate the estimation of the parameters of this signal.

**2.4. AWG transfer characteristic reconstruction**

In [2] is shown how to estimate the input code from the reconstructed output signal of the AWG without any a-priori information. The multi-sine fitting algorithm is used to estimate amplitude, frequency and phase parameters of the reconstructed signal. This information is used to infer the theoretical codes corresponding to the reference signal in the ZCTS  $t_i$ ,  $i=1, \dots, N$ . The reconstructed AWG samples are associated with their theoretical codes. In the case more samples are acquired for the same code, the mean value is considered. The result defines the static characteristic of the AWG.

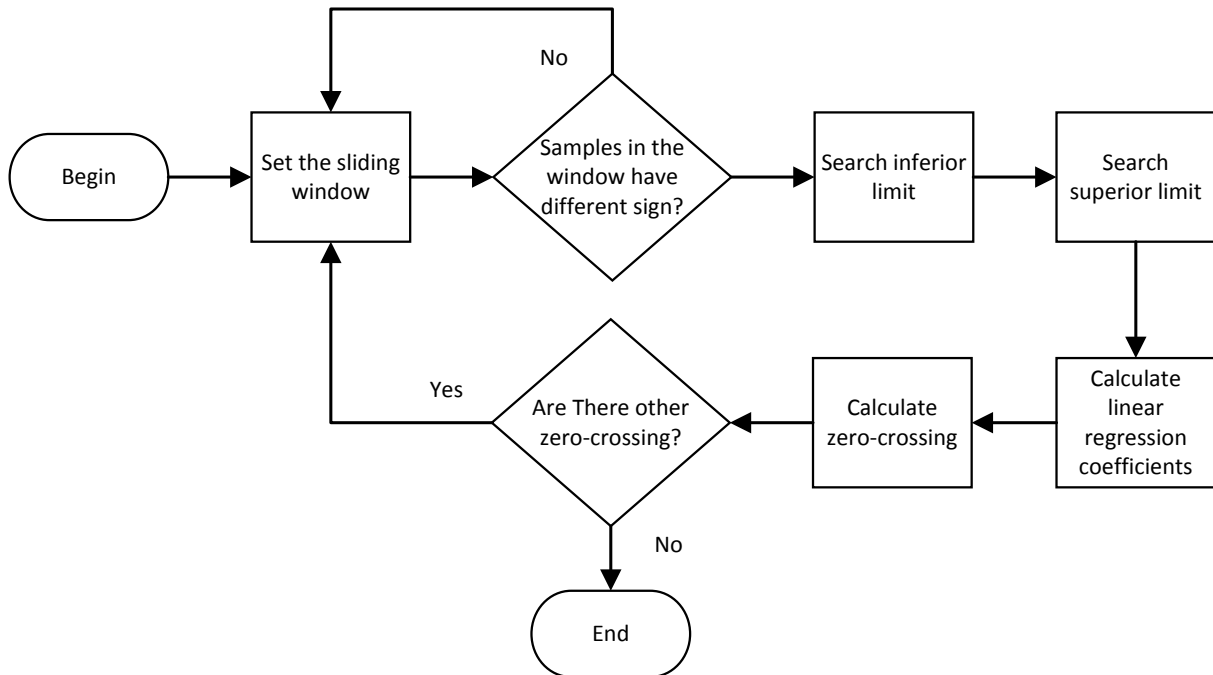


Fig.3. New method for ZCTS estimation.

**3. Numerical Tests**

Numerical tests are developed in MatLab environment in order to validate the proposed methods. Preliminarily, numerical tests are devoted to establishing the influences of the digitalization system parameters on the multi-sine fitting algorithm and on the proposed zero-crossing method. In the following, all the tests

refer to: (i) reference signal with amplitude 1.0 V and frequency 7 kHz, (ii) AWG set to generate sinusoid signal with amplitude 0.1 V and frequency 17 Hz, and (iii) resulting signal digitalized at the sampling frequency of 1 MHz. The ratio between the reference and the resulting signal amplitude is 10 and the ratio between the reference and the resulting signal frequency is 411.7, according with the criteria of the previous section.

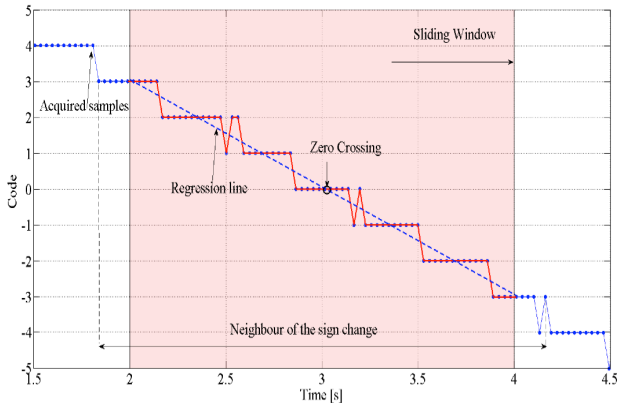


Fig.4. Zero crossing estimation by the proposed method.

### 3.1. Multi-sine fitting

Numerical tests are developed to determine the minimum number of bits of the ADC suitable for the multi-sine fitting algorithm. For each imposed number of bit, 200 tests are repeated with random phase of the reference and AWG signals. White Gaussian noise is also superimposed on the resulting signal before its acquisition with the ADC. The signal-to-noise ratio imposed is equal to 65 dB. Fig.5 shows the trend of the mean value and standard deviation of the error in the amplitude estimation of the reference signal versus the number of bits. The mean value of the error decreases with the increasing of the number of bits. For a number of bits higher than 7 the mean value error is quite constant and is lower than  $0.21 \cdot 10^{-5}$  V, and the standard deviation is  $1.23 \cdot 10^{-5}$  V. Fig.6 shows the trend of the mean value and standard deviation of the error in the phase estimation of the reference signal versus the number of bits. Also in this case the mean value and the standard deviation of the error decreases with the increasing of the number of bits. The mean value is lower than  $0.3 \cdot 10^{-5}$  rad and the standard deviation is lower than  $1.5 \cdot 10^{-5}$  rad for a number of bits equal or greater than 7.

Fig.7 shows the trend of the error in the phase estimation of the reference signal in the case a delay occurs between the reference signal directly acquired and that acquired after the differential amplifier. The delay taken into examination is included in the range [10, 250] ns, that is typical delay introduced by hardware [12],[13]. The error is included in the range [ $4.4 \cdot 10^{-4}$ ,  $110.0 \cdot 10^{-4}$ ] rad and it is at least ten times higher than the error introduced by the multi-sine fitting algorithm.

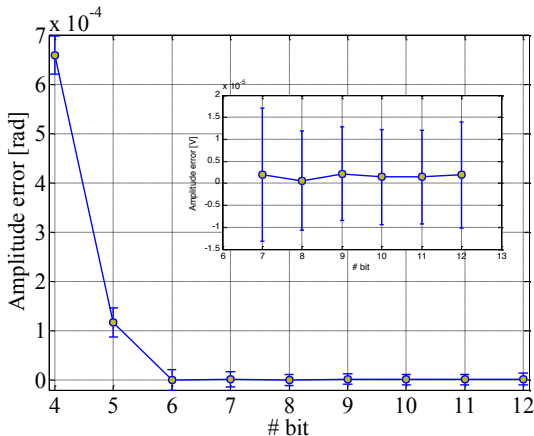


Fig. 5. Mean value and standard deviation of the error in the amplitude estimation of the reference signal versus the number of bits for 200 tests.

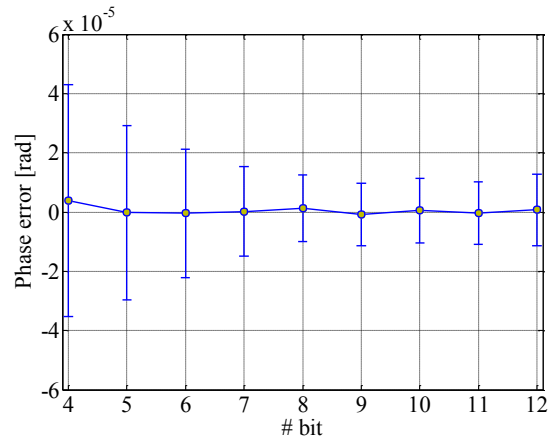


Fig. 6. Mean value and standard deviation of the error of the phase estimation of the reference signal versus the number of bits for 200 tests.

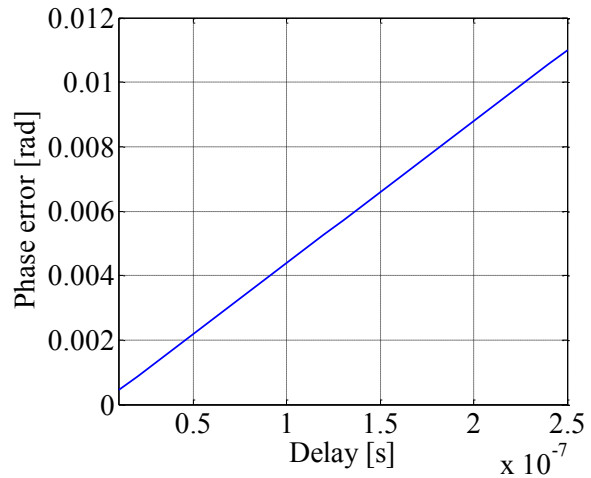


Fig. 7. Error trend in the phase estimation between the reference signal and that acquired after the differential amplifier.

### 3.2. Zero-crossing method

The estimation error of the zero crossing time instant causes the amplitude error of the reconstructed AWG output signal. Preliminary tests are devoted to determine the minimum number of bit of the ADC that permits accurate estimation of the zero crossing. The difference of two sinusoidal signals with amplitudes 1.0 V and 0.1 V and different phase and frequency is taken into consideration. The phase of each signal is randomly generated. Fig. 8 shows the mean value and the standard deviation of the error of the zero-crossing time instant versus the number of bits. The maximum error is lower than  $1.4 \cdot 10^{-7}$  s that is lower than the sampling period used in the tests. The performances of the improved method are compared with that of the zero-crossing detection method used in [2]. The latter detects the first sign change in the samples as zero crossing. Fig. 9 shows the mean value and the standard deviation of the error of the zero-crossing time instant versus the number of bits. The error is always positive and the mean value versus the number of bits is in the neighbour of  $0.5 \cdot 10^{-6}$  s, which is half of the sampling period, but it is ten times greater than the error of the improved method (Fig. 8). For the sake of completeness, the comparison with other zero-crossing method is considered. In [23] is proposed a zero-crossing detection method based on algebraic derivative approach in the frequency domain that provides a detector signal which is equal to zero when the signal has no intersection with real axis and has a peak when a zero crossing occurs. Fig.10 shows the mean value and the standard deviation of the error of the zero-crossing time instant versus the number of bits in the case of method [23]. The

mean value and the standard deviation of the error are compatible with the sampling period, but, also in this case, it is ten times greater than the error of the proposed improved method.

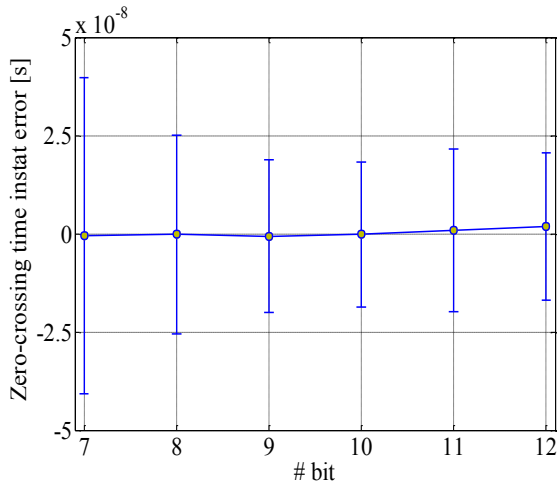


Fig. 8. Mean Value and standard deviation of the error in the zero-crossing time instant estimation for the proposed method versus the number of bits for 200 tests.

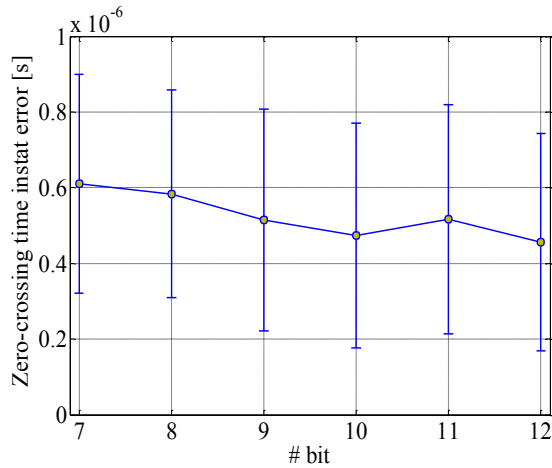


Fig. 9. Mean Value and standard deviation of the error in the zero-crossing time instant detection for the method [2] versus the number of bits for 200 tests.

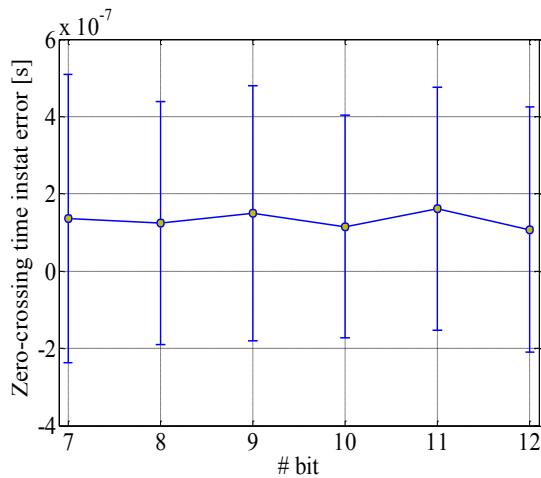


Fig. 10. Mean Value and standard deviation of the error in the zero-crossing time instant detection for the method [23] versus the number of bits for 200 tests.

The transfer characteristic of the 12-bit resolution Tektronix AWG2021 [5] is simulated by a 5<sup>th</sup> order polynomial function. 10 acquisitions of 4 MSamples of the resulting signal obtained by the proposed method are considered and analysed. The mean value of the results of each acquisition is considered for the evaluation of each code. In the tests, the typical parameters of low resolution digitalizing system, as 8 bit oscilloscope, is taken into consideration. In particular, effective 6 bit amplitude resolution [27] is assumed and SNR equal to 65 dB.

Fig. 11 shows the estimated non-linearity of the transfer characteristic of the AWG under test. Fig.12 shows the difference between the estimated characteristic and the imposed one. The error is included in the range [-0.4, 0.4] LSB of the AWG under test and is due to the noise superimposed on the signal. Tests are devoted to investigating the influence of the propagation delay between the reference signal and the resulting signal. A delay of 50 ns, 150 ns, and 250 ns is imposed. The reconstruction error of the AWG transfer characteristic is shown in Fig 13. The error increases as the delay increases. In particular, for a delay of 250 ns the reconstruction error is higher than 5 LSB of the AWG under test for the central codes.

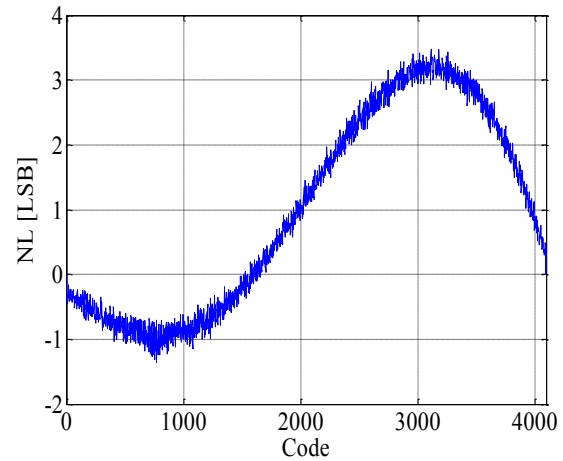


Fig. 11. Estimated non-linearity of the AWG transfer characteristic under test.

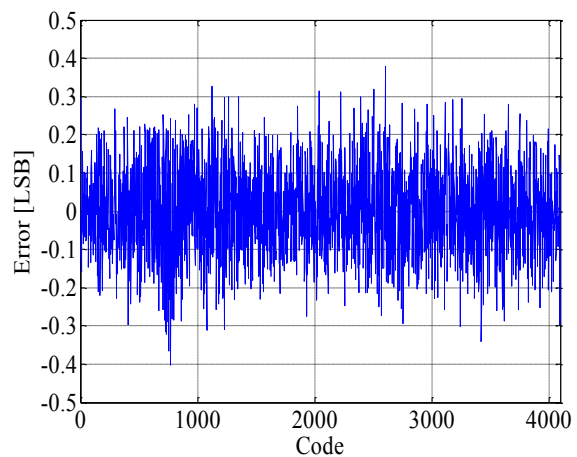


Fig.12. Difference between the non-linearity estimated by the proposed method and the imposed one.

### 3.3. AWG static characterization



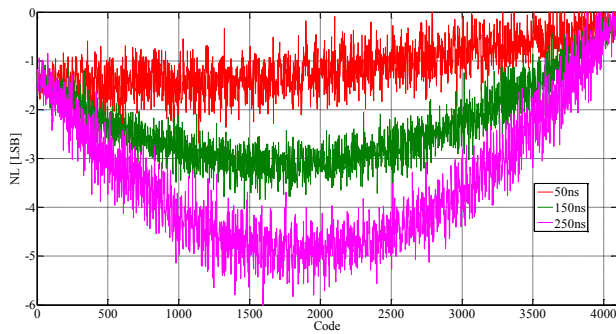


Fig. 13. Reconstruction error of the AWG static characteristic for a delay of 50 ns, 150 ns and 250 ns.

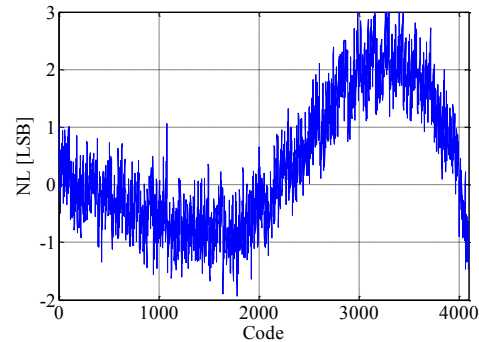


Fig. 15. Measured non-linearity of the AWG2021 by the proposed method.

#### 4. Experimental tests

The experimental tests are performed by considering the AWG Sony/Tektronix 2021 as device under test. The reference signal is generated by Tektronix AFG3022C whose output section is equipped with 14-bit DAC and Bessel cut-off filter. The differential amplifier Tektronix ADA400 is used to obtain the resulting signal that is digitalized by oscilloscope Tektronix TDS7404B characterized by 8-bit resolution. The non-linearity trend of the AWG2021 is evaluated by generating the saw-tooth signal with the amplitude 0.1 V and frequency 17 Hz. The output signal is digitalized by the data acquisition board National Instrument NI6211, characterized by with 16-bit resolution. The nonlinearity is evaluated as the difference between the acquired samples related to the ramp and the theoretical ramp that best fits the samples. The trend of the resulting nonlinearity is shown in Fig. 14. Fig. 15 shows the static characteristic of the AWG2021 evaluated by the proposed method. The comparison between Fig 14 and Fig. 15 highlights that the shape and the amplitude of the non-linearity is the same.

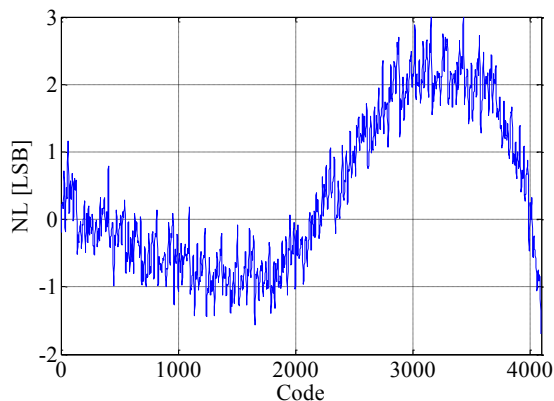


Fig. 14. Measured non-linearity of the AWG2021 by direct acquisition

#### 5. Conclusions

In the paper an improved method for the accurate static characterization of the AWG is proposed. The method is based on the analysis of the resulting signal obtained as the difference between the AWG output and the reference signal. It overcomes the problems arising from the delay introduced by the differential amplifier implementing the difference between the two signals, and the jitter and other noise sources affecting the detection of the ZCTS.

The results of the test show that the mean value and the standard deviation of the error for the estimation of the reference signal parameters decrease with the increasing of the amplitude resolution of the acquisition system. With resolution higher than 6-bit the mean value and the standard deviation of the errors are approximately constant. The non linearity of the AWG is estimated with error included in the range [-0.4, 0.4] LSB of 12 bit DAC of the output section of the AWG, in the case the resulting signal is digitalized by 6 bit ADC.

The comparison of the experimental results obtained by the proposed procedure and by the direct acquisition of the AWG output signal by a 16 bit resolution ADC show that the shape and the amplitude of the estimated non linearity are the same.

#### Acknowledgement

The Author would like to thank Prof. Domenico Grimaldi for his guidance and suggestions in the realization of this paper. He has continually discussed with the Author about all the aspects of the research providing important advice in the realization of the tests.

This is an Open Access article distributed under the terms of the Creative Commons Attribution Licence



#### References

- Baccigalupi, A., D'Arco, M., Liccardo, A. & Vadursi, M. Test equipment for DAC's performance assessment: Design and characterization. *IEEE Trans. Instrum. Meas.* **59**, 1027–1034 (2010).
- Baccigalupi, A., Carni, D. L., Grimaldi, D. & Liccardo, A. Characterization of arbitrary waveform generator by low resolution and oversampling signal acquisition. in *Measurement: Journal of the International Measurement Confederation* **45**, 2498–2510 (2012).
- Baccigalupi, A., D'Arco, M., Liccardo, A. & Vadursi, M. Implementation of high resolution DAC test station: A contribution to draft standard IEEE P1658. in *Proc. of XIX IMEKO World Congress* **1**, 275–280 (2009).
- Carni, D. L. & Grimaldi, D. Spectral test of DAC using over sampling and low resolution ADC. in *Proc. of 16th IMEKO TC4 Int. Symp.: Exploring New Frontiers of Instrum. and Methods for Electrical and Electronic Measurements* 1076–1081 (2008).
- Carni, D. L. & Grimaldi, D. Static and dynamic test of high resolution DAC based on over sampling and low resolution ADC. *Meas. J. Int. Meas. Confed.* **43**, 262–273 (2010).
- Di Nisio, A., Giaquinto, N. & Savino, M. Loop-back linearity test of ADCs and DACs: Measuring simultaneously ADC and DAC nonlinearities by means of dithering and maximum likelihood estimation. in *Proc. of I2MTC 2009 - International Instrumentation*

- and Measurement Technology Conference 856–859 (2009).
7. E., Balestrieri; P., Daponte; S., Moisa; S., R. SOME CRITICAL NOTES ON DAC FREQUENCY DOMAIN SPECIFICATIONS. in *IMEKO WORLD CONGRESS* (2006).
  8. Sekerák, M., Michaeli, L., Liptak, J. & Šaliga, J. New concept for DAC testing under dynamic condition by the comparison with reference voltage. in *Proc. of 22nd International Conference Radioelektronika (RADIOELEKTRONIKA)* 261–264 (2012).
  9. Ting, H. W., Chang, S. J. & Huang, S. L. A design of linearity built-in self-test for current-steering DAC. *J. Electron Test* **27**, 85–94 (2011).
  10. Xuan-Lun, Huang; Jiun-Lang, H. An ADC/DAC loopback testing methodology by DAC output offsetting and scaling. in *VLSI Test Symposium (VTS)* (2010).
  11. Ihs, H., Arabi, K. & Kaminska, B. Testing digital to analog converters based on oscillation-test strategy using sigma-delta modulation. in *Proceedings - IEEE International Conference on Computer Design: VLSI in Computers and Processors* (1998).
  12. Texas Instruments. Triple, Wideband, Voltage-Feedback Operational Amplifier with Disable OPA3690. 1–30 (2010).
  13. AnalogDevices. High Bandwidth , Bidirectional 65 V Difference Amplifier AD8216 \* Product Page Quick Links. (2015).
  14. Carni, D. L. & Fedele, G. Multi-Sine Fitting Algorithm enhancement for sinusoidal signal characterization. *Comput. Stand. Interfaces* **34**, 535–540 (2012).
  15. Carni, D. L. & Grimaldi, D. Characterization of high resolution DAC by DFT and sine fitting. in *Proc. of IEEE Instrumentation and Measurement Technology Conference*, 1250–1253 (2009).
  16. Carni, D. L. & Fedele, G. Improved evaluation of initial condition for the multi-sine fitting algorithm. in *Proc. of the 5th IEEE International Workshop on Intelligent Data Acquisition and Advanced Computing Systems: Technology and Applications, IDAACS* 492–495 (2009).
  17. Ardeleanu, A. S. & Ramos, P. M. Real time PC implementation of power quality monitoring system based on multiharmonic least-squares fitting. *Metrol. Meas. Syst.* **18**, 543–554 (2011).
  18. Ramos, P. M., Janeiro, F. M. & Radil, T. On the use of multi-harmonic least-squares fitting for THD estimation in power quality analysis. *Metrol. Meas. Syst.* **19**, 295–306 (2012).
  19. Carni, D. L. & Grimaldi, D. Comparative analysis of different acquisition techniques applied to static and dynamic characterization of high resolution DAC. in *19th IMEKO World Congress 2009* **1**, 285–289 (2009).
  20. Cadzow, J. A. Minimum  $\ell_1$ ,  $\ell_2$ , and  $\ell_\infty$  Norm Approximate Solutions to an Overdetermined System of Linear Equations. *Digit. Signal Process.* **12**, 524–560 (2002).
  21. Yu, L. & Zhou, X. in *Instrumentation, Measurement, Circuits and Systems* (ed. Zhang, T.) **127 AISC**, 509–517 (Springer Berlin Heidelberg, 2012).
  22. Basu, B. & Basu, M. Predictive zero-crossing detection algorithm by time localised iterative least-square technique. in *Proc. of 14th European Conference on Power Electronics and Applications* 1–7 (2011).
  23. Fedele, G., Chiaravalloti, F. & Join, C. An algebraic derivative-based approach for the zero-crossings estimation. in *17th European Signal Processing Conference* 2455–2459 (2009).
  24. Mendonca, T. R. F., Pinto, M. F. & Duque, C. A. Least squares optimization of zero crossing technique for frequency estimation of power system grid distorted sinusoidal signals. in *11th IEEE/IAS International Conference on Industry Applications (INDUSCON)* 1–7 (2014).
  25. Zhao, S., Zhou, C. & Qiao, C. Zero crossing algorithm for time delay estimation. in *Proc. of IEEE 11th International Conference on Signal Processing (ICSP)* 65–69 (Nanjing University of Aeronautics and Astronautics, 2012).
  26. Alegria, F. C. Precision of the sinefitting-based total harmonic distortion estimator. *Metrol. Meas. Syst.* **23**, 37–46 (2016).
  27. Tektronix. TDS7000 Series Digital Phosphor Oscilloscopes (TDS7104 & TDS7054) Service Manual. Available at: <http://www.tek.com/oscilloscope/tds7054-manual/tds7000-series-service-manual>.